Ionic strength effect on molecular structure of hyaluronic acid investigated by flow field-flow fractionation and multiangle light scattering

Bitnara Kim, Sohee Woo, Young-Soo Park, Euijin Hwang & Myeong Hee Moon

Analytical and Bioanalytical Chemistry

ISSN 1618-2642
Volume 407
Number 5

Anal Bioanal Chem (2015)
407:1327-1334
DOI 10.1007/s00216-014-8379-2

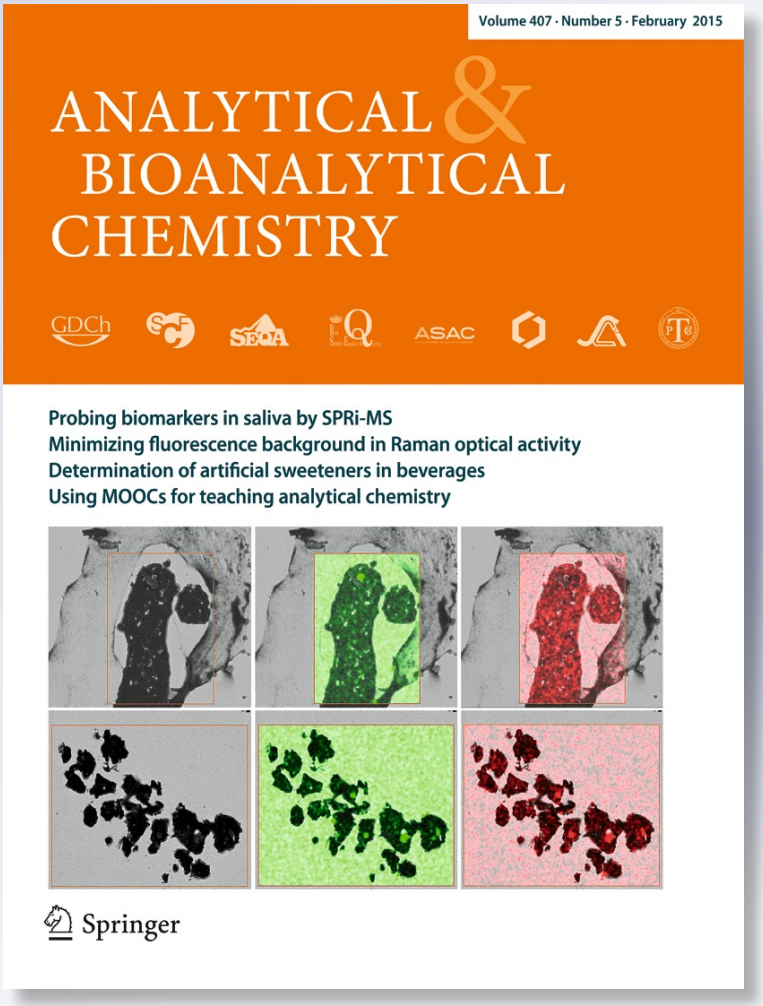

Springer

Anal Bioanal Chem (2015) 407:1327–1334
DOI 10.1007/s00216-014-8379-2

RESEARCH PAPER

Ionic strength effect on molecular structure of hyaluronic acid investigated by flow field-flow fractionation and multiangle light scattering

Bitnara Kim · Sohee Woo · Young-Soo Park · Euijin Hwang · Myeong Hee Moon

Received: 31 July 2014 / Revised: 22 September 2014 / Accepted: 28 November 2014 / Published online: 27 December 2014

Abstract This study describes the effect of ionic strength on the molecular structure of hyaluronic acid (HA) in an aqueous solution using flow field-flow fractionation and multiangle light scattering (FlFFF-MALS). Sodium salts of HA (NaHA) raw materials (~2×10^6 Da) dispersed in different concentrations of NaCl prepared by repeated dilution/ultrafiltration procedures were examined in order to study conformational changes in terms of the relationship between the radius of gyration and molecular weight (MW) and molecular weight distribution (MWD) of NaHA in solution. This was achieved by varying the ionic strength of the carrier solution used in a frit-inlet asymmetrical FlFFF (FIAF4) channel. Experiments showed that the average MW of NaHA increased as the ionic strength of the NaHA solution decreased due to enhanced entanglement or aggregation of HA molecules. Relatively large molecules (greater than ~5 MDa) did not show a large increase in RMS radius value as the NaCl concentration decreased. Conversely, smaller species showed larger changes, suggesting molecular expansion at lower ionic strengths. When the ionic strength of the FlFFF carrier solution was decreased, the HA species in a salt-rich solution (0.2 M NaCl) underwent rapid molecular aggregation during FlFFF separation. However, when salt-depleted HA samples (I=4.66~0.38 mM) were analyzed with FFF carrier solutions of a high ionic strength, the changes in both molecular structure and size were somewhat reversible, although there was a delay in correction of the molecular structure.

Keywords Sodium hyaluronate · Flow field-flow fractionation · Multiangle light scattering · FlFFF-MALS · Ionic strength effect

Introduction

Hyaluronic acid (HA or hyaluronan) is a linear polysaccharide with a disaccharide repeating unit composed of β-D-glucuronic acid and *N*-acetyl-β-D-glucosamine. It is found in the skin, heart, muscles, synovial fluid, eye vitreous, and in rooster combs [1–5]. HA is a polyelectrolyte due to the presence of a carboxylic group in each repeating unit and typically occurs in the body as a sodium salt (NaHA). HA has a number of functions in vivo such as joint lubrication, control of tissue hydration, and wound healing. Solutions of NaHA also have versatile utility in ophthalmic surgery, arthritis treatment, and as fillers for facial wrinkle treatment [4–8]. NaHA is generally believed to form an expanded random coil structure under normal physiological conditions [4, 9–11]. Elongation of the NaHA chain structure in solution is caused by electrostatic repulsion among the carboxylic groups. In the presence of salt (e.g., a NaCl solution), the negative charge of the carboxylic group is shielded by cations. This shielding reduces electrostatic repulsions, resulting in the formation of compact rather than expanded coils, which thus decreases the hydrodynamic size of the molecule [5, 12]. For pharmaceutical and cosmetic applications, raw NaHA materials are typically obtained from rooster combs or microbiological cultures and are processed in order to reduce the MW range and allow for usage in specific applications. The purification process of NaHA often includes repeated dilution and ultrafiltration. Since NaHA molecular

Electronic supplementary material The online version of this article (doi:10.1007/s00216-014-8379-2) contains supplementary material, which is available to authorized users.

B. Kim · S. Woo · M. H. Moon (✉)
Department of Chemistry, Yonsei University, Seoul 120-749, South Korea
e-mail: mhmoon@yonsei.ac.kr

Y.-S. Park · E. Hwang
Department of Biotechnology, Shinpoong Pharmaceutical Co. Ltd., Ansan, Kyeonggi-Do 748-31, South Korea

chains can interact with each other upon changes in the local environment, such as hydration, salt concentration, or hydrogen bonding between NaHA chains, the molecular structure of NaHA is more complicated in an extracellular matrix (a crowded environment with surrounding molecules and salts) than in aqueous solution. In addition, it is known that high-MW NaHA chains (greater than ~10 MDa) entangle with each other even at low concentrations in solution and form compact structures [4, 10].

Studies on the molecular structure of HA and their interactions have been widely performed in aqueous solutions by varying salt concentration, salt composition, or presence of sugars. These studies were based on viscometric analysis in relation to the MW values of HA [5, 13–15] or light scattering analysis to determine MW and conformational information [13, 16]. While these methods have sound theories for determining the molecular structures of polymers from experimental data, HA molecules of very high MW with broad MWD are often complicated to analyze without size sorting. Size exclusion chromatography (SEC) can provide size separation of broad MW HA materials prior to on-line viscometric or multiangle light scattering (MALS) [16]. However, ultrahigh MW (UHMW) HA materials are beyond the capacity of SEC due to the lack of relevant packing materials with sufficient pore sizes to handle these large species and the possible shear-induced degradation of HA chains.

Flow field-flow fractionation (FlFFF) is a powerful technique that has been utilized to separate and characterize water-soluble macromolecules in conjunction with MALS [17–20] due to its unique ability to separate large macromolecules in an open channel. FlFFF separation is carried out in an empty, thin, rectangular-shaped channel by employing two different flow streams: migration flow to drive sample components along the channel axis to the detector and crossflow moving across the flat channel perpendicular to migration flow in order to retain the sample molecules within the channel. Separation of macromolecules or nanoparticles occurs in increasing size order since smaller species, which diffuse faster, are elevated at a higher equilibrium height against the channel wall and so migrate at a higher flow stream path of the parabolic flow pattern compared to larger species. FlFFF-MALS, especially with the use of a frit-inlet asymmetrical FlFFF (FIAF4) channel design, has been utilized for the size separation and characterization of UHMW NaHA materials [21–24]. The FIAF4 channel provides hydrodynamic relaxation of the sample components while they are being injected into the channel by a compressing action of the high-speed frit flow from a small inlet frit located at the beginning of the channel inlet toward the channel wall [25]. This channel design bypasses the typical focusing/relaxation of AF4 channel systems and reduces the occurrence of unwanted sample-wall interactions caused by the stoppage of migration flow during the focusing period. However, a degree of initial band broadening is inevitable in the FIAF4 design.

In this study, conformational change, MW variation, and intermolecular entanglement and disentanglement of raw NaHA materials as a function of changes in ionic strengths of both NaHA and carrier solution of FlFFF were examined using FIAF4-MALS. NaHA samples were prepared from a raw NaHA material (Mw ~2×10^6 Da) using repeated dilution/ultrafiltration processes in order to reduce the ionic strength of the NaHA solution and by resalinization. Our studies focused on the change in average MW of NaHA at low ionic strength and conformational change in the large MW regime of NaHA in terms of the ionic influences that cause electrostatic repulsions between/within NaHA molecules and result in the expansion of coils and/or entanglement.

Experimental

Materials and reagents

Five NaHA samples (Raw, cRaw, UF3, UF5, and Final) were prepared in accordance with the schemes shown in Fig. 1 using materials from Shinpoong Pharmaceutical Company, Ltd. (Ansan, Korea). The raw NaHA material was obtained from rooster combs, and the four other processed samples were obtained by repeated dilution and ultrafiltration processes of the raw material. Detailed information about the NaHA samples is listed in Table 1. A brief explanation of sample preparation is as follows: The raw NaHA material was

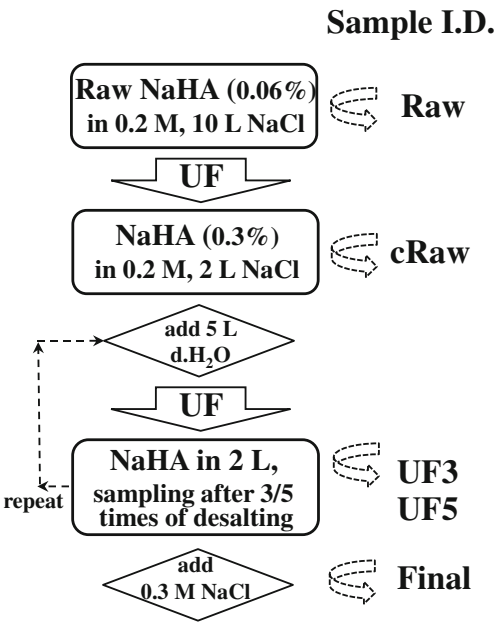

Fig. 1 Schemes for purification and resalination of raw NaHA materials along with the sample identification assigned according to the sampling stage

Table 1 Calculated weight average (Mw) and number average (Mn) molecular weight, RMS radius in weight average (Rw) and number average (Rn), and the slope values of the logarithmic plot of RMS vs. MW for the NaHA samples during purification

Sample ID treatment % NaHA	Raw raw material 0.06 %	cRaw UF concentration ~0.3 %	UF3 Dil/UF 3 times ~0.3 %	UF5 Dil/UF 5 times ~0.3 %	Final NaCl addition ~0.3 %
NaCl in sample (M)	0.2 M, 10 L	0.2 M, 2 L	4.66×10^{-3}	3.81×10^{-4}	0.3
Mw (10^6 g/mol)	2.19±0.14	2.11±0.07	2.89±0.14	3.24±0.14	2.40±0.13
Mn (10^6 g/mol)	1.88±0.06	1.79±0.02	1.69±0.10	1.91±0.10	1.98±0.09
Polydispersity	1.17±0.09	1.18±0.03	1.71±0.14	1.70±0.04	1.21±0.04
Rw (nm)	170.4±5.5	168.0±4.4	208.1±4.3	221.3±7.1	193.6±6.2
Rn (nm)	155.5±6.8	153.7±6.2	151.6±8.1	169.4±8.4	172.2±7.2
Slope	0.48±0.05	0.48±0.02	0.42±0.03	0.36±0.06	0.48±0.06

dispersed in 10 L of 0.2 M NaCl solution at a concentration of 0.06 % (designated as "Raw" in Table 1). Next, "cRaw" was prepared by reducing the volume of Raw to 2 L using ultrafiltration (UF) with a polyethersulfone (PES) membrane filter (300 kDa pore size). The ionic strength of cRaw was maintained (I=0.2 M), but the concentration of NaHA was expected to be 0.3 %. "UF3" was prepared by repeating the dilution/ultrafiltration process three times; 5 L of distilled water was added to cRaw, and then the solution was filtered using the same type of membrane filter (300 kDa) until 2 L of solution remained (I=4.7 mM). "UF5" (I=0.38 mM) was produced after five rounds of the aforementioned dilution/UF process. The sample "Final" was made by adding NaCl to UF5 to a total concentration of 0.30 M NaCl.

FlFFF-MALS-DRI

The FlFFF channel used for this study had a FIAF4 design [25]. This channel was assembled by modifying the inlay of an Eclipse® channel LC from Wyatt Technology Europe GmbH (Dernbach, Germany). The channel inlay used as the depletion wall was modified by inserting a ceramic inlet frit at the beginning end of a polycarbonate inlay cut into an FIAF4 channel type. A ceramic inlet frit (35×18×7 mm) was cut with a semi-circular beginning and was embedded into the polycarbonate inlay utilized as the depletion wall of the AF4 channel system as shown in Fig. S1 in the Electronic Supplementary Material (ESM). A tubing port was drilled 3 mm from the round side of the inlet frit so that a Teflon tubing (i.d. 0.03 in.) could be inserted to deliver sample flow into the channel. The dimensions of the channel space were as follows: a tip-to-tip length of 26.5 cm, a trapezoidal design with a breadth of 1.8-0.4 cm, an inlet frit length of 3.5 cm, and a spacer (Mylar) thickness of 195 μm. The lengths of both triangular ends of the trapezoidal channel were 1.8 and 0.4 cm for the inlet and outlet ends, respectively. A composite regenerated cellulose (CRC) UF membrane, Ultracel® 20 kDa (pore size) from Millipore Corp. (Billerica, MA, USA), was placed above the stainless steel (SS) frit at the accumulation wall. Between the Ultracel® membrane and the SS frit, a polypropylene backing material was positioned to protect the Ultracel® membrane from deformation caused by permeation of the carrier solution through the large pores of the SS frit surface. Carrier solutions for FlFFF were deionized water containing 0.1 M NaCl and 0.02 % NaN_3 as a bactericide. When analyzing the influence of ionic strength of the FFF carrier solution on the molecular structures of different NaHA samples, the NaCl concentration was varied from 0.2 to 0.001 M. Prior to use, all carrier solutions were filtered through a PVDF membrane filter with 0.1 μm pores.

The FIAF4 channel utilized hydrodynamic relaxation such that sample injection and relaxation were continuous without stoppage in migration flow. This continued flow was obtained by applying a high-speed (normally 10~20 times faster than the sample injection flow rate) frit flow to push the incoming sample components from the channel inlet toward the accumulation wall in order to achieve relaxation. Sample injection was performed at 0.1 mL/min using a Model SP930 HPLC pump from Young-Lin Co. (Seoul, Korea) via a model 7725i loop injector (Rheodyne, Cotati, CA, USA). Frit flow was delivered from a model 1260 Infinity HPLC pump from Agilent Technologies (Palo Alto, CA, USA), which was controlled by the Eclipse Separation System for AF4 (Wyatt Technology Europe GmbH). The latter device controlled both the outflow rate and the crossflow rate, of which the latter was programmed to decrease during FIAF4 separation. For both flows (sample flow and frit flow), PEEK inline filter units (VVLP membrane with 0.1 μm pores) from Wyatt Technology Europe GmbH were utilized for solvent filtration. During flow programming, the crossflow rate and the frit flow rate were set to be identical so that the sample flow rate and the injection flow rate were the same. Programming of the crossflow rate utilized multistep linear decay beginning at 2.0 mL/min (maintained for 4 min) and then linearly decreasing to 0.5 mL/min over 5 min, to 0.1 mL/min over 2 min, and finally to 0.02 mL/min over 5 min. The rate was then

maintained at 0.02 mL/min until the completion of FIAF4 separation. The drift in the differential refractive index (DRI) baseline during flow programming was adjusted with each blank run before or after the sample run by using ASTRA software.

Detection of NaHA was achieved with a DAWN-DSP multiangle light scattering (MALS) detector at a wavelength of 632.8 nm, followed by determination of the DRI at 658 nm with an Optilab T-rEX detector (both from Wyatt Technology, Santa Barbara, CA, USA). Calibration and normalization of the MALS detector were performed using the method described in an earlier report [26]. The d*n*/d*c* value of the NaHA sample was measured to be 0.149 with the Optilab T-rEX DRI detector using ASTRA software from the manufacturer. Data collection and MW calculation were performed using ASTRA software from Wyatt Technology. For data calculations, a third-order polynomial fit based on the Berry method of the Debye plot was selected for calculation of the MW of NaHA materials. LS signals at 38°, 44°, 50°, 57°, 64°, 72°, and 81° from MALS were selected from the detector angles. For each sample run, three replicate FFF-MALS runs were made.

Results and discussion

Differences in the molecular weights and structures of the five NaHA samples with varying NaCl concentrations (0.3 to 3.8 × 10^{-4} M) were examined by FIAF4-MALS-DRI using 0.1 M NaCl solution as a carrier liquid for FIAF4 separation. Figure 2a shows the comparison of the fractograms (based on the light scattering (LS) signal detected at 90° from MALS) obtained with the samples Raw and cRaw along with the MALS-DRI calculated MW values at each time point. The superimposed linear plot represents the linear decay pattern of the crossflow rate during separation. Although the NaHA concentration of cRaw was five times higher than that of Raw, because the two samples were dispersed in the same NaCl concentration (0.2 M), they should have possessed the same molecular weight distribution (MWD) unless aggregation was induced during concentration. The weight average molecular weights (Mw) of the two samples, as shown in Table 1, were nearly the same (2.19±0.14 and 2.11± 0.07 MDa). Additionally, the cumulative MWD plots shown in Fig. 2b are very similar each other, representing that there was no significant difference in population of large MW molecules. The conformation plots (the logarithmic plot of the root-mean-square (RMS) radius (or r_g, radius of gyration) vs. MW) superimposed in Fig. 2b show the same slope value (0.48), which suggests that the NaHA molecules were relatively expanded (0.33 for sphere, 0.5~0.6 for linear random coil, and 1 for rigid rod [27]). The consistent increase in RMS radii across the range of MW supports the idea that the NaHA molecules were not aggregated and did not change in conformation during concentration up to 0.3 % NaHA. The ionic strength (I=0.1 M) of the FlFFF carrier solution shown in Fig. 2 was comparable to the concentration used to analyze NaHA materials in previous studies [22, 23]. In this study, NaCl was selected instead of $NaNO_3$ in order to reduce any influence from anionic differences on structural variation. In order to determine the influence of anions in the carrier solution on the molecular structure of NaHA, cRaw was analyzed with a 0.1 M $NaNO_3$ solution as a carrier liquid for FlFFF for comparison. The calculated Mw value was 2.01± 0.09 MDa. This value was not significantly different from that obtained with 0.1 M NaCl. The comparison of fractograms and calculated Mw values obtained in the two carrier solutions is shown in ESM Fig. S2.

When dilution/UF processes were applied to cRaw, the NaHA molecular structure and Mw were significantly changed. The three LS fractograms in Fig. 3a appear to be

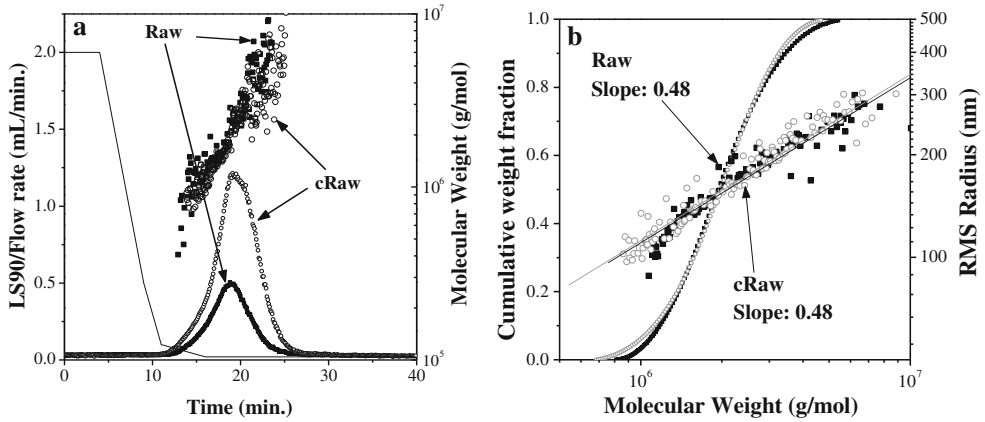

Fig. 2 **a** FIAF4/MALS fractograms of the NaHA samples before and after concentration (Raw and cRaw samples) along with calculated MW values, and **b** cumulative MW distribution (MWD) curves superimposed with the conformation plots (log RMS radius vs. log MW). Analysis conditions for FlFFF: sample flow and outflow rate were set at 0.1 mL/min, crossflow rate (set to be same as frit flow rate) was linearly decreased from 2.0 mL/min as shown in panel a (see "Experimental" section)

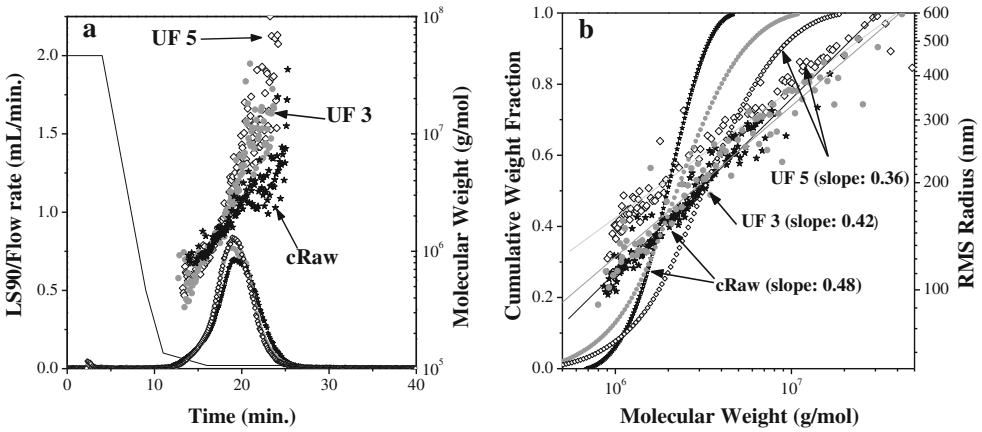

Fig. 3 **a** Fractograms of UF3 and UF5 superimposed with that of cRaw obtained under the analysis conditions used in Fig. 2, and **b** cumulative MWD and conformation plots

similar. However, the calculated MW values of the samples UF3 and UF5 at each time point exhibited steep increases in retention time after 20 min (above 2~3 MDa) compared to that of cRaw. Because the NaCl concentrations in the NaHA samples were decreased from 0.2 M (cRaw) to 4.66 mM and 0.38 mM for UF3 and UF5, respectively, it can be posited that the NaHA chains were exposed to a lower ionic strength. Therefore, they are expected to be more expanded as a result of the increase in electrostatic repulsions between carboxylic groups (due to the decreased charge screening effect). Average MW values of the NaHA samples after depletion of NaCl are shown in Table 1 to significantly increase from 2.11 MDa (cRaw) to 2.89 and 3.24 MDa for UF3 and UF5, respectively. These increases in Mw result from the formation of greater MW fractions (greater than ~8 MDa). However, UHMW fractions of UF3 and UF5 eluted much earlier than HA molecules in the same MW region of cRaw. For example, the retention time of 8×10^6 Da molecules from UF3 and UF5 eluted at 20–22 min, while cRaw molecules of the same size eluted at ~24 min. As the salt concentration decreased, the effects of charge screening decreased and electrostatic repulsion between carboxylic groups increased. Both of these changes may have led to the expanded configuration of HA. If the HA molecules simply expanded or elongated at low ionic strength solutions, their retention time should have increased in the FlFFF channel due to the shape effect. However, UHMW fractions had shorter retention times, suggesting that aggregates or supramolecular structures were present at low ionic strength conditions. This can be explained by the increased Mw values of each desalted sample in addition to the decrease in the conformational slope values to 0.42 and 0.36 for UF3 and UF5, respectively, as shown in the conformation plots in Fig. 3b. While large molecules did not show large differences in RMS radius with a decrease in NaCl concentration, the RMS radius values of relatively smaller species (lesser than ~5 MDa) increased appreciably, evidence of molecular expansion at lower ionic strengths.

While the experiments in Fig. 3 were obtained at a carrier solution with an ionic strength much higher than those of the sample solutions (0.1 M NaCl vs. 4.66 and 0.38 mM NaCl), the results in Fig. 3 may not be truly representative of the actual MW distribution or the structures since the NaHA molecules contained in the low ionic strength solutions were analyzed under higher ionic strength conditions. However, the experimental results shown in Fig. 3 do suggest that changes in HA molecular structure were not immediately reversed during the FlFFF experiments (~20 min).

In order to examine the ionic strength effect of the carrier solution on the structure of NaHA molecules, cRaw and UF5 were chosen for comparison. These samples were tested by varying the concentration of NaCl in the carrier solution of FlFFF. Carrier solutions of four different NaCl concentrations (0.2, 0.1, 0.01, and 0.001 M) were utilized to examine the changes in retention and MW distribution of cRaw (Fig. 4) and UF5 (ESM Fig. S3). When the ionic strength of the FlFFF carrier solution was 0.2 M NaCl, which was the same concentration as cRaw, NaHA molecules eluted smoothly with an increase in MW, as shown in Fig. 4a. This was similar to the elution pattern obtained with a 0.1 M NaCl solution (Fig. 2a). Among the calculated values of Mw (1.90 vs. 2.11 MDa), Rw (162.0 vs. 168.0 nm), and the conformational slope (0.49 vs. 0.48) obtained at carrier solutions of the two different NaCl concentrations in Table 2 (cRaw), the only significant difference was for Mw. The Mw value measured with 0.2 M NaCl solution decreased by approximately 10 %. These data showed that sufficient ionic strength (≥0.1 M) yielded stabilization of electrostatic repulsions, resulting in consistent molecular structures and Mw. When the ionic strength of the FlFFF carrier solution was decreased to 0.01 M and 0.001 M NaCl (Fig. 4a), significant decreases in the retention time were observed (see the LS signals shifted to shorter time scales). Additionally, the Mw value increased (to 3.79 and 5.57 MDa, respectively, Table 2 (cRaw)) and the conformation slope decreased (0.42 and 0.33, respectively). The peak shift toward shorter retention time scale observed with the NaHA

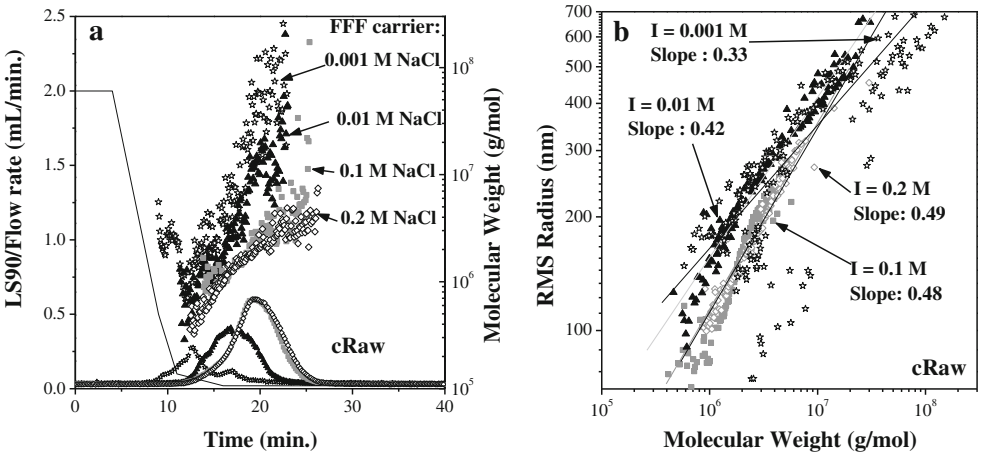

Fig. 4 Effect of ionic strength of FFF carrier solution on retention of cRaw (dispersed in 0.2 M NaCl): **a** superimposed fractograms of cRaw obtained at 0.2, 0.1, 0.01, and 0.001 M NaCl solutions, and **b** the comparison of the conformational slope values from the plots of RMS radius vs. MW

molecules at a carrier solution with lower ionic strength (Fig. 4a) was caused by the elevated migration of NaHA molecules from the channel wall due to the increased double layer thickness above the channel membrane. The calculated Mw value of cRaw (originally in 0.2 M NaCl solution) obtained with the 0.001 M NaCl carrier solution (Table 2 (cRaw)) was 5.57 MDa, much larger than the 3.24 MDa of the sample UF5, for which analysis was carried out in a 0.1 M NaCl solution (as listed in Table 1). This difference suggests that a carrier solution with a low ionic strength greatly influences the molecular structure of NaHA in less than 10 min, which was the time period between sample injection and the beginning of elution in FlFFF. Increased interaction of NaHA molecules with membrane surface due to the change in zeta potential may influence the observed increase in aggregation. However, return of the molecular structure and disaggregation were rather slow when salt-depleted NaHA molecules (UF5) were injected into carrier solutions of higher ionic strength. In addition, the depletion of sodium ions around NaHA molecules in a diluted (0.001 M) carrier solution should be fast enough to induce aggregation of HA molecules. Similar analysis of UF5 at carrier solutions with different ionic strengths (ESM Fig. S3) showed that the Mw value decreased as the salt concentration in the carrier solution increased (as listed in Table 2 (UF5)). However, the Mw decreased to 2.59 MDa with 0.2 M NaCl solution. This value was still larger than the molecular weight obtained for cRaw analyzed with a 0.2 M NaCl solution (1.90 MDa). These results show that some structural changes were irreversible, and that a period of time was required for significantly entangled/aggregated NaHA molecules at a very low ionic strength to resume their original structures when they were injected into carrier solutions of higher ionic strengths.

After the repeated dilution/UF steps of the purification process, resalination was carried out by adding NaCl to the nearly desalted HA solution (the same as UF5) to make a 0.3 M NaCl solution (as represented in Fig. 1). This "Final" sample was analyzed under the same conditions used in the

Table 2 Calculated Mw and Mn values of cRaw and UF5 under carrier solutions with different NaCl concentration obtained by FIAF4-MALS-DRI

NaCl in FFF carrier (M)	0.2	0.1	0.01	0.001
cRaw				
Mw (10^6 g/mol)	1.90±0.09	2.11±0.07	3.79±0.14	5.57±0.34
Mn (10^6 g/mol)	1.65±0.01	1.79±0.02	2.10±0.07	2.00±0.09
Polydispersity	1.15±0.06	1.18±0.03	1.81±0.10	2.79±0.12
Rw (nm)	162.0±4.7	168.0±4.4	295.0±15.5	245.3±17.2
Rn (nm)	146.9±8.5	153.7±6.2	233.9±12.9	210.6±16.8
Slope	0.49±0.03	0.48±0.02	0.42±0.03	0.33±0.02
UF5				
Mw (10^6 g/mol)	2.59±0.15	3.24±0.14	3.92±0.08	4.29±0.12
Mn (10^6 g/mol)	1.60±0.02	1.91±0.10	2.22±0.10	1.47±0.04
Polydispersity	1.61±0.09	1.70±0.04	1.76±0.06	2.93±0.09
Rw (nm)	234.6±7.4	221.3±7.1	301.6±14.1	300.7±18.0
Rn (nm)	184.5±8.5	169.4±8.4	261.4±16.4	213.7±9.9
Slope	0.41±0.02	0.36±0.06	0.32±0.01	0.31±0.01

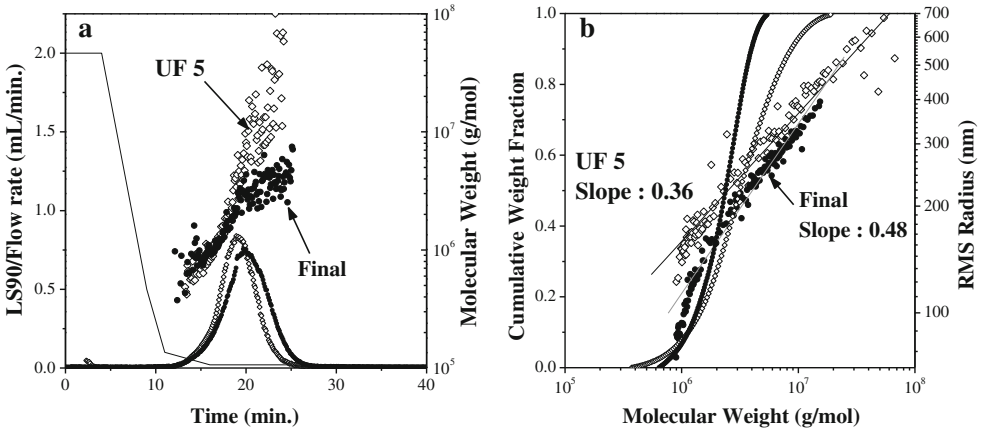

Fig. 5 Effect of resalination of UF5 on the MW and structure of NaHA molecules: **a** comparison of retention profiles between UF5 and Final (resalinized to 0.3 M NaCl) obtained at the carrier solution used in Fig. 3, and **b** cumulative MWDs along with conformation plots

experiment shown in Fig. 2. Figure 5 shows the differences in retention and MW distribution before (UF5) and after resalination (Final), and that the conformation slope returned to 0.48 (from 0.36). Comparing the calculated MW values of the UF5 and Final sample species eluted for 20 min illustrated an evident increase in retention time of molecular species larger than ~3 MDa in the "Final" sample. This could be caused by disaggregation followed by restructuring into an extended conformation. Conformation plots in Fig. 5b show that the RMS radius values for species smaller than ~5 MDa of the "Final" sample appeared to be smaller than those of UF5, supporting the belief that relatively smaller HA molecules (lesser than ~5 MDa) become more compact in size at higher ionic strength conditions due to the decreased charge screening effect. However, the decrease in the RMS radius values of larger species (>10 MDa) at a higher ionic strength carrier solution was not as large as that observed for smaller species. This demonstrates that the increase in conformational slope value (from 0.36 to 0.48) was largely caused by the change in conformation of the smaller MW species (lesser than ~5 MDa) into more compact geometries at a higher ionic strength. The Mw value of the "Final" sample was reduced to 2.40 MDa (in Table 1) but was still higher than the molecular weight of cRaw (2.11 MDa) obtained under the same run conditions. This suggests the presence of some irreversible structures. However, it cannot exclude the possibility that the difference in Mw values can originate from a slow kinetic effect of "Final" sample during the period of separation.

Conclusions

This study performed systematic evaluation of the influences of ionic strength of the sample dispersion and the carrier solutions used for FlFFF separation on molecular size and conformation of HA molecules. Characterization was completed with on-line measurement of MALS-DRI. When the NaCl concentration of NaHA sample solutions decreased, NaHA molecules became more extended and formed a random coil structure due to the decreased charge screening effect. This led to an increase in electrostatic repulsion between the carboxylic groups of HA molecules. In addition, UHMW species were formed as the ionic strength of either the sample dispersion or carrier solution decreased, leading to a systematic increase in Mw. While increases in the RMS radius values of relatively smaller species (lesser than ~5 MDa) were observed with salt-depleted (or low ionic strength) NaHA samples in a 0.1 M NaCl carrier solution and with the cRaw sample (I=0.2 M) in carrier solutions of low ionic strengths, the RMS radius values of UHMW species that emerged at low ionic strength conditions did not change significantly. It was assumed that HA molecules smaller than ~5 MDa were significantly influenced by the ionic environment; therefore, their structures became more expanded at a low ionic strength. Conversely, larger species were not as dramatically influenced. Conformation slope values decreased with decreasing ionic strength, indicating that UHMW species originated from the formation of aggregates or entangled structures at low ionic strengths. In addition, although NaHA molecules rapidly underwent structural changes and aggregation when they were injected into FFF carrier solutions of lower ionic strengths, the return to the original molecular structure was comparatively slow when molecules were relocated to higher salt environments from a salt-depleted status.

Acknowledgments This study was supported by a grant from the National Research Foundation (NRF) funded by the Korea government (NRF-2010-0014046).

References

1. Cortivo R, Brun P, Rastrelli A, Abatangelo G (1991) Biomaterials 12: 727–730
2. Prestwich GD, Marecak DM, Marecek JF, Vercruysse KP, Ziebell MR (1998) J Control Release 53:93–103

3. Iqbal Z, Midgley JM, Watson DG, Karditsas SD, Dutton GN, Wilson W (1997) Pharm World Sci 19:246–250
4. Cowman MK, Matsuoka S (2005) Carbohydr Res 340(5):791–809
5. García-Abuín A, Gómez-Díaz D, Navaza JM, Regueiro L, Vidal-Tato I (2011) Carbohydr Polym 85:500–505
6. Saari H, Konttinen YT, Santavirta S (1989) Med Sci Res 17:99–101
7. Takahashi R, Al-Assaf S, Williams PA, Kubota K, Okamoto A, Nishinari K (2003) Biomacromolecules 4:404–409
8. Mengher LS, Pandher KS, Bron AJ, Davey CC (1986) Br J Ophthalmol 70:442–447
9. Cleland RL (1977) Arch Biochem Biophys 180:57–68
10. Necas J, Bartosikova L, Brauner P, Kolar J (2008) Vet Med 53:397–411
11. Horkay F, Basser PJ, Londono DJ, Hecht AM, Geissler E (2009) J Chem Phys 131:184902
12. Kobayashi Y, Okamoto A, Nishinari K (1994) Biorheology 31:235–244
13. Sheehan JK, Arundel C, Phelps CF (1983) Int J Biol Macromol 5: 222–228
14. Fouissac E, Milas M, Rinaudo M (1993) Macromolecules 26:6945–6951
15. Mendichi R, Šoltés L, Giacometti Schieroni A (2003) Biomacromolecules 4:1805–1810
16. Cowman MK, Liu J, Li M, Hittner DM, Kim JS (1998) In: Laurent TC (ed) The chemistry, biology, and medical applications of hyaluronan and its derivatives. Portland, London
17. Wittgren B, Wahlund KG (1997) J Chromatogr A 760:205–218
18. Wittgren B, Wahlund KG (1997) J Chromatogr A 791:135–149
19. Leeman M, Wahlund KG, Wittgren B (2006) J Chromatogr A 1134: 236–245
20. Wittgren B, Borgstorm J, Piculell L, Wahlund KG (1998) Biopolymers 45:85–96
21. Lee H, Cho IH, Moon MH (2006) J Chromatogr A 1131:185–191
22. Moon MH, Shin DY, Lee N, Hwang E, Cho IH (2008) J Chromatogr B 864:15–21
23. Kwon JH, Hwang E, Cho IH, Moon MH (2009) Anal Bioanal Chem 395:519–525
24. Moon MH (2010) J Sep Sci 33:3519–3529
25. Moon MH, Kwon H, Park I (1997) Anal Chem 69:1436–1440
26. Lee H, Kim H, Moon MH (2005) J Chromatogr A 1089:203–210
27. Cervantes J, El-Shehawy AA et al (2005) Current topics. In: Bregg RK (ed) Polymer research. Nova, New York